How to cite: *Angew. Chem. Int. Ed.* **2023,** *62,* e202303151
doi.org/10.1002/anie.202303151

Coordination Chemistry

# Fine-Tuning Redox Properties of Heteroleptic Molybdenum Complexes through Ligand-Ligand-Cooperativity

*Benedict J. Elvers,* Sebastian Pätsch, Siva S. M. Bandaru, Vera Krewald, Carola Schulzke, and Christian Fischer**

*Dedicated to Professor Joachim Heinicke valuing his lifetime achievement in phosphorous and nitrogen-based chemistry.*

**Abstract:** Heteroleptic molybdenum complexes bearing 1,5-diaza-3,7-diphosphacyclooctane ($P_2N_2$) and non-innocent dithiolene ligands were synthesized and electrochemically characterized. The reduction potentials of the complexes were found to be fine-tuned by a synergistic effect identified by DFT calculations as ligand-ligand cooperativity via non-covalent interactions. This finding is supported by electrochemical studies combined with UV/Vis spectroscopy and temperature-dependent NMR spectroscopy. The observed behavior is reminiscent of enzymatic redox modulation using second ligand sphere effects.

The active sites of many metalloenzymes benefit from controlled reaction environments, which often positively influence the overall reaction by interactions of or with the second ligand sphere.[1] Attempts to chemically model these effects have resulted in the field of metal-ligand cooperativity (MLC)[2] and in stabilization strategies for supramolecular complex assembly via ligand-ligand interaction (LLI) utilizing non-covalent interactions (NCI).[3] Various types of MLC have been reported, from internal pH modulation,[4] pendant reactive sites,[2d,5] and structural stabilization of distinct coordination geometries,[6] to redox non-innocence.[7] Modeling the intricate influence of the second ligand sphere on the redox properties in a small metal ion bearing compound is challenging. Subtle redox potential changes of transition metal complexes are achieved most often by substituent variation in the ligand backbones and by distortion of the coordination geometry through a rigid ligand backbone, thereby altering the electronic structures of the complexes.[6,8]

A much less common and decidedly more difficult approach towards redox tuning exploits intramolecular interactions in the second ligand sphere. For instance, hydrogen bonds from urea-derived tripodal ligands were used to stabilize an oxo ligand and tune its reactivity in high-valent complexes.[9] As a side effect, the hydrogen bonds indirectly modulate the electron density at the transition metal and thus its redox properties. In a more directed approach, hydrogen bonding was used to obtain "pseudo" chelating ligands, changing their bite angle and, consequently, the overall electronic structures.[3d,e,g,10] In nickel complexes with one multidentate ligand, a varied chirality in the ligand backbone altered the exhibited π–π interactions, resulting in a slightly different geometry and thus modulated redox potential.[11] This observation could be considered a rare case of cooperativity in the outer coordination sphere between the substituents of one ligand. With regard to metal-ligand cooperativity, two types of ligands known for their MLC ability are particularly noteworthy: 1,5-diaza-3,7-diphosphacyclooctanes (short: $P_2N_2$) and ene-dithiolates (or: dithiolenes), see Figure 1. The $P_2N_2$ ligand is often associated with proton reduction/hydrogen oxidation reactions in which its pendant amines and internal proton

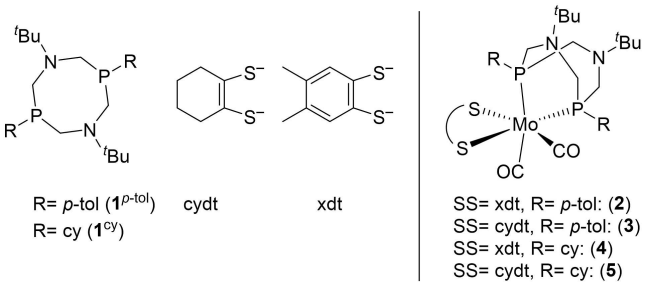


***Figure 1.*** Chemical structures of the investigated molybdenum monodithiolene complexes and their respective ligands (*p*-tol = *p*-tolyl, cy = cyclohexyl). For molecular structures of the four complexes, see Figure S1.

[*] Dr. B. J. Elvers, S. Pätsch, Dr. S. S. M. Bandaru, Prof. Dr. C. Schulzke, Dr. C. Fischer
Bioinorganic Chemistry, Institute for Biochemistry, University of Greifswald
17489 Greifswald (Germany)
E-mail: benedict.elvers@uni-greifswald.de
christian.fischer@uni-greifswald.de

Dr. B. J. Elvers
Biophysical Chemistry, Institute for Biochemistry, University of Greifswald
17489 Greifswald (Germany)

Prof. Dr. V. Krewald
Theoretical Chemistry, Institute for Chemistry, TU Darmstadt
64287 Darmstadt (Germany)

relays are utilized.[12] The dithiolene ligand is a notorious *non-innocent* ligand known for its ability to influence the redox properties of the coordinated metal directly.[13]

While optimizing the properties of molybdenum complexes with varying combinations of these two types of ligands (Figure 1) with the aim to balance their electronic properties, stabilities, reactivities, and catalytic abilities, an unexpected yet rather remarkable synergistic effect of the two ligands was noticed.

Complexes with monodithiolene ligands are known to exhibit rather close-lying potentials upon reduction.[13e,14] In molybdenum complexes **2** and **3** with a ligand sphere that combines two distinct dithiolene ligands with the novel $P_2^{p\text{-}tol}N_2^{tBu}$ ligand ($\mathbf{1}^{p\text{-}tol}$), a highly unusual modulation of the redox behavior was observed. In the voltammograms of **2** and **3** (Figure 2), the two half-step potentials ($E_{1/2}$) at ≈−2 V are almost collapsed, essentially beginning to merge into one 2e⁻ event. Differential pulse voltammetry (DPV) verified that indeed two 1e⁻ reduction events take place (Figure S2). To assess the contribution of the $P_2N_2$ ligand to the observed phenomenon, a second set of monodithiolene complexes, **4** and **5**, was synthesized using the known $P_2^{cy}N_2^{tBu}$ ($\mathbf{1}^{cy}$).[15] For these complexes, no such collapse was observed (Figure S3 and Table 1). In the oxidative regions, the typical 2e⁻ oxidation is found for each of the four complexes. As described earlier,[13e] this is followed by a chemical reaction (*EC*-mechanism), releasing CO and yielding a solvent-coordinated complex. Further proof for the latter is provided by the XRD (X-ray diffraction) molecular structure of [Mo(CH$_3$CN)$_3$(cydt)($P_2^{p-tol}N_2^{tBu}$)]$^{2+}$ (**6**) (Figure S4).[16]

Density functional theory (DFT) calculations were performed to better understand the distinct electrochemical

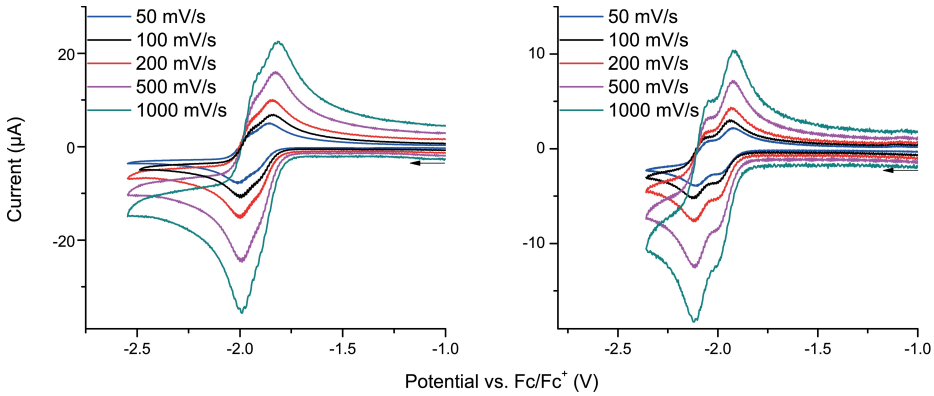


***Figure 2.*** Close-up of the scan rate dependent cyclic voltammetry of [Mo(CO)$_2$(dt)($P_2^{p\text{-}tol}N_2^{tBu}$)] (dt = xdt (**2**), left; dt = cydt (**3**), right). Measurements were performed in CH$_3$CN using 0.1 M (*n*-Bu$_4$N)(PF$_6$) as supporting electrolyte. Potentials are summarized in Table 1. Full cyclic voltammograms are shown in Figure S3.

***Table 1:*** Half step potentials ($E_{1/2}$), cathodic peak potential ($E_{pc}$), and anodic peak potential ($E_{pa}$) of [Mo(CO)$_2$(dt)($P_2^{p\text{-}tol}N_2^{tBu}$)], dt = xdt (**2**), dt = cydt (**3**) and [Mo(CO)$_2$(dt)($P_2^{cy}N_2^{tBu}$)], dt = xdt (**4**), dt = cydt (**5**). Measurements were performed in CH$_3$CN at room temperature using 0.1 M (*n*-Bu$_4$N)(PF$_6$) as a supporting electrolyte at 100 mV s$^{-1}$.

| | (**2**) | (**3**) | (**4**) | (**5**) |
|---|---|---|---|---|
| $E_{1/2}{}^1$ | −1.971 V[a] | −2.097 V[a] | −2.124 V | −2.246 V |
| $E_{pc}{}^1$ | −1.993 V[a] | −2.130 V[a] | −2.163 V | −2.278 V |
| $E_{pa}{}^1$ | −1.949 V[a] | −2.064 V[a] | −2.085 V | −2.215 V |
| $\Delta U^1$ | 44 mV[a] | 66 mV[a] | 78 mV | 63 mV |
| $E_{1/2}{}^1$(DPV) | −1.971 V | −2.120 V | – | – |
| $E_{1/2}{}^2$ | −1.871 V[a] | −1.965 V[a] | −1.882 V | −1.966 V |
| $E_{pc}{}^2$ | −1.902 V[a] | −1.998 V[a] | −1.922 V | −2.002 V |
| $E_{pa}{}^2$ | −1.839 V[a] | −1.932 V[a] | −1.841 V | −1.929 V |
| $\Delta U^2$ | 63 mV[a] | 66 mV[a] | 81 mV | 73 mV |
| $E_{1/2}{}^2$(DPV) | −1.889 V | −1.995 V | – | – |
| additional. $E_{pc}$ | – | −0.521 V | −0.423 V | −0.584 V |
| $E_{1/2}{}^3$ | – | 0.021 V | 0.098 V | −0.047 V |
| $E_{pc}{}^3$ | – | −0.011 V | 0.073 V | −0.090 V |
| $E_{pa}{}^3$ | 0.232 V | 0.052 V | 0.122 V | −0.003 V |
| $\Delta U^3$ | – | 63 mV | 49 mV | 88 mV |
| $\Delta$ ($E_{1/2}{}^1 - E_{1/2}{}^2$) | 100 mV | 132 mV | 242 mV | 280 mV |
| $\Delta$ ($E_{1/2}{}^1$(DPV) − $E_{1/2}{}^2$(DPV)) | 82 mV | 123 mV | – | – |
| $\Delta$ ($E_{1/2}{}^1 - E_{1/2}{}^2$)$_{calc}$[b] | 159 mV | 201 mV | 227 mV | 265 mV |

[a] Half-step potentials and peak potentials roughly estimated by turning points in the cyclic voltammograms. [b] Calculated as final single point energy differences from DFT calculations with the TPSSh functional.

behavior of the $P_2N_2$ coordinated complexes starting with coordinates obtained from XRD measurements.[17] In the optimized structures of singly and doubly reduced forms of **2** and **3**, the dithiolene ligands xdt and cydt, respectively, are bent at the two sulfur atoms, leading to a stacked arrangement with the adjacent *p*-tolyl substituents of the $P_2N_2$ ligand (Figure 3 and S5). At first deemed a case of an optimization slip-up based on using the BP86 functional, this type of structure is, in fact, consistently found also with other density functionals in which the NCIs in the second ligand sphere are captured by the respective dispersion correction according to Grimme (D3zero, see Computational Details). For the singly reduced complex $\mathbf{2}^{1-}$ the density functionals BP86, TPSSh,[18] and PBE0[19] give comparable results. The BP86 and TPSSh functionals produce almost identical, acute bending angles (151° and 153°), whereas with PBE0, a slightly less bent structure results (159°, Figure 3). The TPSSh density functional produced the best agreement with experimental IR and UV/Vis spectra of the neutral species **2** (Figures S6–S8 and Table S2). In the following, hence, only the results based on TPSSh calculations are discussed.

The bending of the dithiolene (Mo-SS-$dt_{backbone}$) was observed to be most pronounced with an aromatic ring system on both $P_2N_2$ and dithiolene ligand ($\mathbf{2}^{1-}$: 151°). It decreases in the order $\mathbf{3}^{1-}$, $\mathbf{4}^{1-}$, and $\mathbf{5}^{1-}$ (163°, 170°, 172°) and is hence the smallest when both ligands are non-aromatic cyclohexyl derivatives. Most notably, the bending positively correlates with the degree of signal merging in the reductive regions of the voltammograms (Figure S10). A similar but decidedly distinct effect was observed for high-valent dithiolene metal complexes and defined as the "folding angle".[20] In that case the dithiolene bending compensates for the electron deficiency by improved S-π-donation. In the present case, the ligand motion (Figure S13 and Table S3) must have a different origin since the d-orbitals are nearly or completely filled.

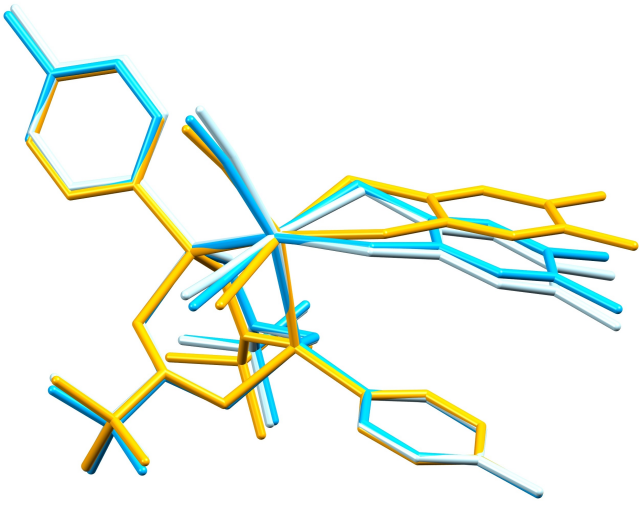

***Figure 3.*** Superposition of singly reduced $[Mo(CO)_2(P_2^{p\text{-}tol}N_2^{tBu})(xdt)]^{1-}$ ($\mathbf{2}^{1-}$) calculated with different density functionals (BP86: light blue; TPSSh: blue; PBE0: orange) in which dispersion is parameterized differently; visualization with Mercury. See Figure S9 for additional perspectives.

In the case of the xdt coordinated complex $\mathbf{2}^{1-}$, the NCI can be best described as parallel offset π-stacking[21] with a distance of 3.9 Å between both arene rings in the computed structures. Replacing the *p*-tolyl group with hydrogen *in silico* leads to a relaxed structure with no dithiolene bend (177°, Figure S11). We can therefore conclude that ligand bending results from a NCI of the dithiolene backbone with the *p*-tolyl substituent. Switching off the dispersion correction during the geometry relaxation of $\mathbf{2}^{1-}$ resulted in a structure without NCI in the second coordination sphere (Figure S12). The difference in energy for $\mathbf{2}^{1-}$ was calculated to be 2.4 kcal mol$^{-1}$ lower for the "stacked" structure, which is in accordance with similar intramolecular London dispersion forces.[11b] The most significant degree of stabilization of the "stacked" structure is seen when both ligands are aromatic ($\mathbf{2}^{1-}$) and decreases with the gradual replacement of the arene groups by cyclohexyl-derived moieties ($\mathbf{3}^{1-}$: 1.7 kcal mol$^{-1}$; $\mathbf{4}^{1-}$: 1.1 kcal mol$^{-1}$; $\mathbf{5}^{1-}$: 1.2 kcal mol$^{-1}$) just as the degree of dithiolene bending does. We note that these minor energy differences should be taken as an indication of the more stable species, not as a quantification of the stabilization energy due to dispersion.

Regarding the experimentally observed near-collapse of the reduction events, the theoretical differences between the potentials for the two reduction steps ($\Delta = (E_{1/2}{}^1 - E_{1/2}{}^2)_{calc}$) can be calculated from final single point energy differences.[22] We find that more closely spaced potentials are correlated with more stabilized dithiolene bending (**2** Δ: 159 mV, **3** Δ: 201 mV, **4** Δ: 227 mV, and **5** Δ: 265 mV) in accordance with the experimental observations (Table 1 and S4).

The character of the HOMO of $\mathbf{2}^{1-}$ is dominated by a Mo-carbonyl π-bonding interaction with some sulfur non-bonding contribution, while the SOMO (LUMO of **2**) is best described as a Mo-dithiolene π-anti-bonding orbital. Despite the bending of the dithiolene ligand, the delocalized π-system consisting of Mo d-orbitals and sulfur and dithiolene carbon p-orbitals remains as intact (see Figure S14–S16) as in comparable complexes.[13e,14] The geometry change and ligand bending is facilitated by molybdenum by decreasing its SOMO contribution via the $d_{x^2-y^2}$ orbital from 12.6 % (non-stacked) to 6.9 % (stacked) while increasing its $d_{xz}$ contribution from 8.2 % (non-stacked) to 14.3 % (stacked) (Table S5). In consequence, the molybdenum orbital share of the SOMO is geometrically linked to the degree of the dithiolene tilt. The $d_{xy}$ orbital contribution to the SOMO (6.5 vs. 6.6 %) remains essentially the same in the distinct geometries. However, the axial donors (CO and P) almost halve their contributions to the SOMO in the "stacked" species (stacked: CO 8.5 %; P 4.2 %; non-stacked: CO 14.1 %, P 6.8 %; Table S7).

The first reduction step is also associated with a change in coordination geometry from trigonal prismatic to octahedral, as was shown before by DFT calculations and reported for related monodithiolene complexes.[13e,14,23] Such a torsion is evident also here from the Bailar-Twist angles[24] of the "stacked" (52.2°) and "non-stacked" (45.2°) structures of $\mathbf{2}^{1-}$ compared to the parent complex (**2**) (3.1°; Table S1). All four complexes investigated here exhibit the same computational geometry change upon reduction. However, only the

$P_2^{p\text{-tol}}N_2^{t\text{Bu}}$ species additionally engage in a significant degree of ligand stacking due to NCIs. Since DFT calculations suggest the stacking interaction to be energetically relatively weak (**2**$^{1-}$: 2.4 kcal, **3**$^{1-}$: 1.7 kcal; Tables S4), it should be rather thermo-responsive. While cooling is expected to stabilize the stacking and support the collapse of the two redox events in the voltammograms, heating should do the reverse. This hypothesis was investigated by temperature-dependent cyclic voltammetry (Figure 4).

Commonly, temperature-dependent cyclic voltammetric studies result in a congruent shift of all signals either up- or down-potential.[25] Here, in contrast, with lower temperatures, the two reductive potentials of **2** and **3** moved towards each other, resulting in a more substantial overlap or even full merge (**2**) of these events and a greater separation at higher temperatures. This observation agrees with the weak NCI between adjacent arenes indicated by DFT calculations as the underlying cause.

With a recently published method for spectral decomposition of spectro-electrochemical UV/Vis data, the time-dependent concentration (Figure S17) and the pure component spectra of all four investigated monodithiolene complexes were extracted including those of their corresponding reduced states that were generated only *in situ* (Figure S18–S21).[13e,26] These spectra were then used to validate the ligand stacking further. For $[Mo(CO)_2(P_2^{p\text{-tol}}N_2^{t\text{Bu}})(xdt)]^{1-}$ (**2**$^{1-}$) (Figure S18), the two bands observed experimentally at 567 nm and 470 nm are better reproduced with the computational transitions as calculated for the "stacked" than for the "non-stacked" species.

For further experimental evidence of the unusual behavior of the compounds' coordination spheres, the complexes were reduced *in situ* and monitored by $^{31}$P NMR spectroscopy. In the case of **3**, $[Co(Cp^*)_2]$ was used as the reducing agent resulting merely in the release of the phosphane ligand. In contrast, when **2** was reacted with $KC_8$ at varying temperatures, two new doublets appeared (in addition to the starting material and free ligand, Figure S22). These exhibit a $^2J_{^{31}P-^{31}P}$ coupling constant of 40.2 Hz that likely corresponds to an octahedral complex with two chemically inequivalent $^{31}$P atoms. NOESY studies were then performed to directly characterize the aromatic rings' interaction. These show a correlation signal (Figure S23 and S24) for the protons of the tolyl residue (≈7.01 ppm) and the xdt ligand (≈7.84 ppm) that is absent in the starting material.

Considering all experimental and DFT data, the observed intramolecular interaction between the dithiolene and the $P_2N_2$ ligand that results in fine-tuning the complexes' redox properties can be described as ligand-ligand cooperativity (LLC) arising from non-covalent interactions. The geometric change in the coordination sphere upon reduction results in spatial proximity of the backbone of the *non-innocent* dithiolene ligand and the substituent on the phosphane ligand. This proximity allows both ligands to interact electronically after a folding motion of the dithiolene. The dithiolene bending and moving away from the equatorial plane likely results in a reduced orbital overlap between sulfur p and molybdenum d orbitals and, hence, a reduced supply of electron density from S to Mo. This would be in accordance with a facilitated reduction of the metal center and a less negative redox potential for the second reduction, as was observed electrochemically. The induced "conversation" between the ligands modulates the electronic structure of the complex, thereby directly influencing the redox properties, as evidenced by the cyclic voltammograms. This type of second ligand sphere interaction of two distinct ligands in a single complex is unprecedented for molecular compounds and may be considered a model system for second coordination sphere effects in metalloenzymes. The detailed understanding of the observed LLC and subsequent redox modulation, as provided herein, should help facilitate the development of new molecular redox catalysts exploiting such second-ligand sphere effects in the future.

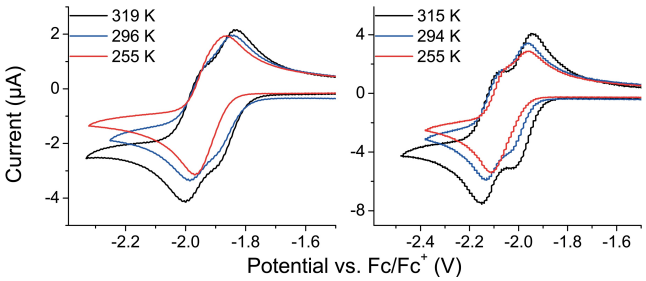


***Figure 4.*** Close-up of the temperature-dependent cyclic voltammetry of **2** (left) and **3** (right) in $CH_3CN$ using 0.1 M ($n$-$Bu_4N$)($PF_6$) as supporting electrolyte.

## Acknowledgements

C.S. gratefully acknowledges general financial support from the DFG (SCHU 1480/4-2). B.J.E. thanks the Deutsche Bundesstiftung Umwelt (DBU, AZ 20018/562) for financial support during his Ph.D. thesis and Prof. Mihaela Delcea for the freedom to pursue independent research. Open Access funding enabled and organized by Projekt DEAL.

## Conflict of Interest

The authors declare no conflict of interest.

## Data Availability Statement

The data that support the findings of this study are available from the corresponding author upon reasonable request.

**Keywords:** Ligand-Ligand Cooperativity · Non-Innocence Ligands · Noncovalent Interactions · Redox Chemistry

[1] a) J. W. Slater, S. C. Marguet, M. E. Gray, H. A. Monaco, M. Sotomayor, H. S. Shafaat, *ACS Catal.* **2019**, *9*, 8928–8942; b) C. Van Stappen, Y. Deng, Y. Liu, H. Heidari, J. X. Wang, Y.

Zhou, A. P. Ledray, Y. Lu, *Chem. Rev.* **2022**, *122*, 11974–12045; c) J. Cupp-Vickery, *Proc. Natl. Acad. Sci. USA* **2000**, *97*, 3050–3055; d) R. G. Hadt, N. Sun, N. M. Marshall, K. O. Hodgson, B. Hedman, Y. Lu, E. I. Solomon, *J. Am. Chem. Soc.* **2012**, *134*, 16701–16716; e) T. P. Warelow, M. J. Pushie, J. J. H. Cotelesage, J. M. Santini, G. N. George, *Sci. Rep.* **2017**, *7*, 1757.

[2] a) C. A. Hunter, H. L. Anderson, *Angew. Chem. Int. Ed.* **2009**, *48*, 7488–7499; b) J. R. Khusnutdinova, D. Milstein, *Angew. Chem. Int. Ed.* **2015**, *54*, 12236–12273; c) J. R. Khusnutdinova, D. Milstein, *Angew. Chem.* **2015**, *127*, 12406–12445 ;.d) M. R. Elsby, R. T. Baker, *Chem. Soc. Rev.* **2020**, *49*, 8871–8250.

[3] a) T. Ohno, S. Kato, *Bull. Chem. Soc. Jpn.* **1974**, *47*, 2953–2957; b) T. Ohno, S. Kato, *Bull. Chem. Soc. Jpn.* **1974**, *47*, 1901–1907; c) H. Sigel, *Pure Appl. Chem.* **1989**, *61*, 923–932; d) J. Meeuwissen, J. N. Reek, *Nat. Chem.* **2010**, *2*, 615–621; e) M. Raynal, P. Ballester, A. Vidal-Ferran, P. W. van Leeuwen, *Chem. Soc. Rev.* **2014**, *43*, 1660–1733; f) P. Dydio, J. N. H. Reek, *Chem. Sci.* **2014**, *5*, 2135–2145; g) J. N. H. Reek, B. de Bruin, S. Pullen, T. J. Mooibroek, A. M. Kluwer, X. Caumes, *Chem. Rev.* **2022**, *122*, 12308–12369.

[4] a) A. D. Wilson, R. H. Newell, M. J. McNevin, J. T. Muckerman, M. Rakowski DuBois, D. L. DuBois, *J. Am. Chem. Soc.* **2006**, *128*, 358–366; b) B. Ginovska-Pangovska, A. Dutta, M. L. Reback, J. C. Linehan, W. J. Shaw, *Acc. Chem. Res.* **2014**, *47*, 2621–2630; c) M. E. Ahmed, S. Dey, M. Y. Darensbourg, A. Dey, *J. Am. Chem. Soc.* **2018**, *140*, 12457–12468; d) Z. Thammavongsy, I. P. Mercer, J. Y. Yang, *Chem. Commun.* **2019**, *55*, 10342–10358.

[5] a) M. Shibasaki, M. Kanai, N. Kato, E. Ichikawa, *Synlett* **2005**, *2005*, 1491–1508; b) R. H. Crabtree, *New J. Chem.* **2011**, *35*, 18–23; c) E. M. Nichols, J. S. Derrick, S. K. Nistanaki, P. T. Smith, C. J. Chang, *Chem. Sci.* **2018**, *9*, 2952–2960; d) T. Chantarojsiri, J. W. Ziller, J. Y. Yang, *Chem. Sci.* **2018**, *9*, 2567–2574; e) M. D. Wodrich, X. Hu, *Nat. Chem. Rev.* **2017**, *2*, 0099; f) J. J. Kiernicki, M. Zeller, N. K. Szymczak, *Inorg. Chem.* **2020**, *59*, 9279–9286.

[6] a) E. I. Solomon, M. D. Lowery, J. A. Guckert, L. B. LaCroix, *Adv. Chem.* **1997**, *253*, 317–330; b) G. Chaka, J. L. Sonnenberg, H. B. Schlegel, M. J. Heeg, G. Jaeger, T. J. Nelson, L. A. Ochrymowycz, D. B. Rorabacher, *J. Am. Chem. Soc.* **2007**, *129*, 5217–5227; c) D. J. Mercer, S. J. Loeb, *Chem. Soc. Rev.* **2010**, *39*, 3612–3620; d) J. Stanek, A. Hoffmann, S. Herres-Pawlis, *Coord. Chem. Rev.* **2018**, *365*, 103–121; e) I. O. Koshevoy, M. Krause, A. Klein, *Coord. Chem. Rev.* **2020**, *405*, 213094; f) H. B. Lee, T. Agapie, *Inorg. Chem.* **2019**, *58*, 14998–15003.

[7] a) O. R. Luca, R. H. Crabtree, *Chem. Soc. Rev.* **2013**, *42*, 1440–1459; b) B. de Bruin, P. Gualco, N. D. Paul in *Ligand Design in Metal Chemistry* (Eds.: M. Stradiotto, R. Lundgren), Wiley, Hoboken, **2016**, pp. 176–204.

[8] a) A. I. Nguyen, J. Wang, D. S. Levine, M. S. Ziegler, T. D. Tilley, *Chem. Sci.* **2017**, *8*, 4274–4284; b) Z. Gordon, M. J. Drummond, E. M. Matson, J. A. Bogart, E. J. Schelter, R. L. Lord, A. R. Fout, *Inorg. Chem.* **2017**, *56*, 4852–4863; c) C. Palopoli, J. Ferreyra, A. Conte-Daban, M. Richezzi, A. Foi, F. Doctorovich, E. Anxolabehere-Mallart, C. Hureau, S. R. Signorella, *ACS Omega* **2019**, *4*, 48–57.

[9] a) T. Taguchi, R. Gupta, B. Lassalle-Kaiser, D. W. Boyce, V. K. Yachandra, W. B. Tolman, J. Yano, M. P. Hendrich, A. S. Borovik, *J. Am. Chem. Soc.* **2012**, *134*, 1996–1999; b) S. A. Cook, A. S. Borovik, *Acc. Chem. Res.* **2015**, *48*, 2407–2414; c) S. A. Cook, E. A. Hill, A. S. Borovik, *Biochemistry* **2015**, *54*, 4167–4180.

[10] a) P. W. van Leeuwen, P. C. Kamer, J. N. Reek, P. Dierkes, *Chem. Rev.* **2000**, *100*, 2741–2770; b) J. Wassenaar, J. N. Reek, *Org. Biomol. Chem.* **2011**, *9*, 1704–1713.

[11] a) O. A. Levitskiy, O. I. Aglamazova, T. V. Magdesieva, *Electrochim. Acta* **2019**, *306*, 568–574; b) O. A. Levitskiy, O. I. Aglamazova, A. V. Dmitrieva, T. V. Magdesieva, *Electrochim. Acta* **2021**, *388*, 138537.

[12] a) M. Rakowski DuBois, D. L. DuBois, *Chem. Soc. Rev.* **2009**, *38*, 62–72; b) M. L. Helm, M. P. Stewart, R. M. Bullock, M. R. DuBois, D. L. DuBois, *Science* **2011**, *333*, 863–866; c) T. Liu, D. L. DuBois, R. M. Bullock, *Nat. Chem.* **2013**, *5*, 228–233.

[13] a) D. V. Fomitchev, B. S. Lim, R. H. Holm, *Inorg. Chem.* **2001**, *40*, 645–654; b) F. J. Hine, A. J. Taylor, C. D. Garner, *Coord. Chem. Rev.* **2010**, *254*, 1570–1579; c) R. Eisenberg, H. B. Gray, *Inorg. Chem.* **2011**, *50*, 9741–9751; d) P. Basu, K. J. Colston, B. Mogesa, *Coord. Chem. Rev.* **2020**, *409*, 213211–213211; e) B. J. Elvers, M. Sawall, E. Oberem, K. Heckenberger, R. Ludwig, K. Neymeyr, C. Schulzke, V. Krewald, C. Fischer, *Chem. Methods* **2021**, *1*, 22–35.

[14] Y. Yan, P. Chandrasekaran, J. T. Mague, S. DeBeer, S. Sproules, J. P. Donahue, *Inorg. Chem.* **2012**, *51*, 346–361.

[15] J. Y. Yang, S. Chen, W. G. Dougherty, W. S. Kassel, R. M. Bullock, D. L. DuBois, S. Raugei, R. Rousseau, M. Dupuis, M. Rakowski DuBois, *Chem. Commun.* **2010**, *46*, 8618–8620.

[16] Deposition Numbers 2238167 (for **2**), 2238168 (for **3**); 2238169 (for **4**), 2238170 (for **5**), and 2238171 (for **6**) contain the supplementary crystallographic data for this paper. These data are provided free of charge by the joint Cambridge Crystallographic Data Centre and Fachinformationszentrum Karlsruhe Access Structures service.

[17] a) A. D. Becke, *Phys. Rev. A* **1988**, *38*, 3098–3100; b) J. P. Perdew, *Phys. Rev. B Condens. Matter* **1986**, *33*, 8822–8824; c) F. Neese, *J. Comput. Chem.* **2003**, *24*, 1740–1747.

[18] a) V. N. Staroverov, G. E. Scuseria, J. Tao, J. P. Perdew, *J. Chem. Phys.* **2003**, *119*, 12129–12137; b) J. P. Perdew, J. Tao, V. N. Staroverov, G. E. Scuseria, *J. Chem. Phys.* **2004**, *120*, 6898–6911; c) K. P. Jensen, *Inorg. Chem.* **2008**, *47*, 10357–10365.

[19] C. Adamo, V. Barone, *J. Chem. Phys.* **1999**, *110*, 6158–6170.

[20] a) J. W. Lauher, R. Hoffmann, *J. Am. Chem. Soc.* **1976**, *98*, 1729–1742; b) H. K. Joshi, J. J. Cooney, F. E. Inscore, N. E. Gruhn, D. L. Lichtenberger, J. H. Enemark, *Proc. Natl. Acad. Sci. USA* **2003**, *100*, 3719–3724; c) J. Yang, J. H. Enemark, M. L. Kirk, *Inorganics* **2020**, *8*, 19.

[21] a) C. R. Martinez, B. L. Iverson, *Chem. Sci.* **2012**, *3*, 2191–2201; b) T. Zhang, J. Vanderghinste, A. Guidetti, S. V. Doorslaer, G. Barcaro, S. Monti, S. Das, *Angew. Chem. Int. Ed.* **2022**, *61*, e202212083.

[22] a) M. Namazian, C. Y. Lin, M. L. Coote, *J. Chem. Theory Comput.* **2010**, *6*, 2721–2725; b) L. Castro, M. Buhl, *J. Chem. Theory Comput.* **2014**, *10*, 243–251; c) B. H. Solis, S. Hammes-Schiffer, *Inorg. Chem.* **2014**, *53*, 6427–6443.

[23] B. J. Elvers, C. Schulzke, C. Fischer, *Eur. J. Inorg. Chem.* **2019**, 2796–2805.

[24] a) P. Ray, N. K. Dutt, *J. Indian Chem. Soc.* **1943**, *20*, 81–92; b) A. Rodger, B. F. G. Johnson, *Inorg. Chem.* **1988**, *27*, 3061–3062.

[25] a) C. Schulzke, *Dalton Trans.* **2005**, 713–720; b) C. Schulzke, *Dalton Trans.* **2009**, 6683–6691; c) N. Chrysochos, M. Ahmadi, S. Wahlefeld, Y. Rippers, I. Zebger, M. A. Mroginski, C. Schulzke, *Dalton Trans.* **2019**, *48*, 2701–2714.

[26] a) M. Sawall, C. Fischer, B. J. Elvers, S. Pätsch, K. Neymeyr, *Anal. Chim. Acta* **2021**, *1185*, 339065; b) S. V. Zade, K. Neymeyr, M. Sawall, C. Fischer, H. Abdollahi, *J. Chemom.* **2022**, *37*, e3453.

Manuscript received: March 6, 2023
Accepted manuscript online: April 14, 2023
Version of record online: May 9, 2023